

Lateral stability analysis of steel tapered thin-walled beams under various boundary conditions

M. Soltani*, S. Asil Gharebaghi**, F. Mohri***

ARTICLE INFO

Article history:

Received:

November 2017.

Revised:

April 2018.

Accepted:

August 2018.

Keywords:

Lateral-Torsional

Buckling (LTB)

Finite Difference Method
(FDM)

Power Series Method
(PSM)

Tapered thin-walled beam

Abstract:

The lateral-torsional buckling of tapered thin-walled beams with singly-symmetric cross-section has been investigated before. For instance, the power series method has been previously utilized to simulate the problem, as well as the finite element method. Although such methods are capable of predicting the critical buckling loads with the desired precision, they need a considerable amount of time to be accomplished. In this paper, the finite difference method is applied to investigate the lateral buckling stability of tapered thin-walled beams with arbitrary boundary conditions. Finite difference method, especially in its explicit formulation, is an extremely fast numerical method. Besides, it could be effectively tuned to achieve a desirable amount of accuracy. In the present study, all the derivatives of the dependent variables in the governing equilibrium equation are replaced with the corresponding forward, central and backward second order finite differences. Next, the discreet form of the governing equation is derived in a matrix formulation. The critical lateral-torsional buckling loads are then determined by solving the eigenvalue problem of the obtained matrix. In order to verify the accuracy of the method, several examples of tapered thin-walled beams are presented. The results are compared with their counterparts of finite element simulations using shell element of known commercial software. Additionally, the result of the power series method, which has been previously implemented by the authors, are considered to provide a comparison of both power series and finite element methods. The outcomes show that in some cases, the finite difference method not only finds the lateral buckling load more accurately, but outperforms the power series expansions and requires far less central processing unit time. Nevertheless, in some other cases, the power series approximation has less relative error. As a result, it is recommended that a hybrid method, based on a combination of the finite difference technique and the power series method, be employed for lateral buckling analysis. This hybrid method simultaneously inherits its performance and accuracy from both mentioned numerical methods.

1. Introduction

Due to efficiency in the increasing stability of structures, reduction in structural weight and cost and the improvements in fabrication process, thin-walled beams with open and variable cross-section are extensively spread in steel structures as beams and columns. Regarding the presence of bending-torsion coupling effect and variable cross-section properties, accurate estimation of lateral buckling loads is complicated.

Therefore, there are a large number of researches devoted to lateral-torsional stability analysis of thin-walled beams. Many numerical techniques such as finite element method or the power series method have been utilized to solve the stability of the thin-walled structures. Consequently, some improvements have been obtained by several authors in the case of non-uniform thin-walled beams with arbitrary cross-section shapes. Closed-form solutions for the flexural and lateral-torsional stability of thin-walled beams have been carried out since the early works of Timoshenko and Gere, 1961 [34], Vlasov, 1962 [35], Chen and Lui, 1987 [11] and Bazant and Cedolin, 1991 [7] for I-beams under some representative load cases. For tapered beams, Brown, 1981 [9] adopted a shell element method to obtain the numerical buckling load of tapered beams. Yang and Yau, 1987 [36] formulated a general finite element model to investigate the instability of a doubly symmetric tapered

* Corresponding Author: Assistant Professor, Department of civil engineering, University of Kashan, Kashan, Iran Email: msoltani@kashanu.ac.ir

** Associate Professor, Civil Engineering Faculty, K.N.Toosi university of Technology, Tehran, Iran .

*** Associate Professor, Université de Lorraine, CNRS, Arts et Métiers ParisTech, LEM3, LabEx DAMAS, F-57000 METZ, France.

I-beam by considering the effect of geometric non-linearity. In the case of stability analysis of thin-walled beam with variable cross-section based on a variational approach, Pasquino and Sciarra, 1992 [27] derived the governing equilibrium equations. Kim and Kim, 2000 [17] proposed a finite element approach for the lateral-torsional buckling and vibration analyses of doubly symmetric I tapered thin-walled beams. Yau, 2006 [37] adopted a finite element procedure to analyze lateral stability behavior of tapered I-beams under torsion moment. In this study, the total potential energy was obtained by discretizing one single beam into three narrow tapered elements. In other words, two flanges and web of each cross-section were considered as a tapered thin-walled beam. Based on the Rayleigh-Ritz method, combined with shell element, a general variational formulation to analyze the lateral-torsional buckling behavior of tapered thin-walled beams with singly symmetric I-section was presented by Andrade and Camotim, 2005 [2] and Andrade *et al.*, 2007 [3]. Erkmén and Mohareb, 2008 [14, 15] adopted the combinations of stationary complementary energy and Koiter's polar decomposition theory to determine a new finite Element model of thin-walled members with open sections for linear buckling analysis. Regarding deformation compatibilities of web and flanges, the total potential energy was obtained by Lei and Shu, 2008 [20] to present a finite Element model for linear lateral stability analysis of web-tapered beams with doubly symmetric I-section. Kurniawan and Mahendran, 2009 [18] presented a finite element technique to study the lateral-torsional and distortional behaviors of simply supported Light Steel Beams (LSBs) under bending loading in which the effect of additional twisting caused by load eccentricity is taken into account. Attard and Kim, 2010 [6] adopted hyperelastic constitutive model to obtain the equilibrium equations and lateral buckling of prismatic beam due to the presence of shear deformation. The exact lateral-torsional stability criterion of cantilever strip beam subjected to combined effects of intermediate and end transverse point loads by means of Bessel functions was proposed by Challamel and Wang, 2010 [10]. Based on determining the total potential energy and employing the Rayleigh-Ritz method, Kabir and Seif, 2010 [16] proposed an analytical method to obtain lateral-torsional buckling load of a beam with I-section and retrofitted using FRP sheets. Asgarian *et al.*, 2013 [5] studied the lateral-torsional behavior of tapered beams with singly-symmetric cross-sections. The equilibrium equation was solved by the power series expansions. This method has been applied to beams where boundary conditions and loads could be arbitrary. Web and flange tapering have also been considered. An analytical technique was proposed by Yuan *et al.*, 2013 [38] to obtain the lateral-torsional buckling load of steel web tapered tee-section cantilevers subjected to a uniformly distributed load and/or a concentrated load at the free end. A non-linear formula based on 1D model for lateral buckling analysis of simply supported tapered beams with doubly symmetric cross-sections was proposed by Benyamina *et al.*, 2013 [8]. Kuś, 2015 [19] investigated a numerical procedure for the lateral buckling stability analysis of beams with doubly-symmetric cross-section. In his work,

the Ritz method has been adopted and the effects of simultaneous changes of the web height and flange width are taken into consideration. Recently, Ruta and Szybinski, 2015 [29] applied Chebyshev series to solve the torsion fourth order differential equation obtained by Asgarian *et al.*, 2013 [5] and also to determine the critical lateral-torsional buckling of simply supported and cantilever beams with arbitrary open cross-sections. Based on non-linear model, Mohri *et al.*, 2015 [24] extended the tangent stiffness matrix and 3D beam element with seven degrees of freedom to the lateral buckling stability of thin-walled beams with consideration of large displacements and initial stresses. The post buckling behavior was measured in the first time and compared to shell elements. Based on Vlasov's assumption, Chen *et al.*, 2016 [12] derived the element stiffness matrix of the pre-twisted thin-walled straight beam with elliptical section and I-cross-section. Effect of uniform Winkler-Pasternak elastic foundation on torsional post-buckling behavior of clamped beam with doubly-symmetric I-section was assessed by Rao and Rao, 2017 [28]. Based on a generalized layered global-local beam (GLGB) theory, Lezgy-Nazargah, 2017 [21] proposed an efficient finite element model for the elastoplastic analysis of beams with thin-walled cross-section. Moreover, a new finite element solution was proposed by Nguyen *et al.*, 2017 [25, 26] for computing lateral-torsional critical loads of FGM thin-walled beams with singly symmetric open-section. Based on the classical energy approach, Chen *et al.*, 2019 [13] suggested a novel technique for estimating the lateral-torsional buckling load of simply supported beam with I-section. In order to investigate the buckling capacity of straight thin-walled box beam (STBB) subjected to an eccentric force, a non-linear theory was developed by Tan and Cheng, 2019 [33]. More recently, Achref *et al.*, 2019 [1] assessed higher buckling and lateral buckling of beams with open cross sections through an analytical technique and finite element solution.

In previous authors' works (Asgarian *et al.*, 2013 [5], Soltani *et al.*, 2014 [30, 31]; Soltani *et al.*, 2019 [32]), the stability and vibration behavior of tapered beams with thin-walled cross-section was comprehensively assessed. For instance, a numerical technique based on the power series expansions of displacement components was employed to simulate the problem (Asgarian *et al.*, 2013 [5], Soltani *et al.*, 2014 [30]), as well as finite element method (Soltani *et al.*, 2014 [31]; Soltani *et al.*, 2019 [32]). Since, the linear stability behavior of beam with thin-walled open cross-section is governed by three fourth-order differential equations coupled in terms of the transverse deflection, the lateral displacement, and the torsion angle, the power series method requires a considerable amount of time to determine explicit expressions of displacement functions. Another numerical method based on the power series expansions to acquire structural stiffness matrices was also proposed by authors to perform lateral stability analysis of non-prismatic members with non-symmetric thin-walled cross-section (Soltani *et al.*, 2014 [31]; Soltani *et al.*, 2019 [32]). It is believed that this finite element solution is a bit faster than PSM. Please refer to Soltani *et al.*, 2019 [32] for more details.

The main purpose of the current paper is to investigate the lateral-torsional buckling behavior of tapered beams with singly-symmetric cross-section under arbitrary loads by an alternative more efficient numerical technique: the finite difference method. In the first stage, the equilibrium differential equation of the non-prismatic beam in terms of twist angle and the related boundary conditions are expressed. In the second stage, the fourth order differential equation and boundary conditions are discretized by FDM. In this regard, the expressions of derivatives of displacement represented in the stability equation are presented based on aforementioned numerical method. Finally, the system of finite difference equations culminates in a set of simultaneous linear equations and the elastic critical lateral buckling loads are calculated by solving an eigenvalue problem of the obtained algebraic system.

In order to demonstrate the accuracy and efficiency of this method, two numerical examples are studied. Different representative load cases and various boundary conditions are considered. The obtained results are compared to finite element simulations using ANSYS software and to other available numerical and analytical benchmark solutions. The stability analysis of uniform members as well as non-uniform ones can be performed through the proposed method. Comments and conclusions are presented towards the end of the manuscript.

2. Lateral Stability Equilibrium Equation for Tapered Beams with Singly-Symmetric Cross-Section

A non-prismatic thin-walled beam with singly-symmetric I section as depicted in Fig. 1a is taken into account. It is contemplated that the beam is made from homogenous and isotropic material with E and G the Young's modulus and shear constant. In the current research, the beam is initially subjected to arbitrary distributed force q_z in z direction along with a line (PP') on the section contour (Fig. 1a). The displacement parameters of thin-walled beams with singly-symmetric cross-section are depicted in Fig. 1b. The shear center C is known by its coordinates $(0, z_c)$ in the reference coordinate system, which is fixed in centroid O . On the section contour, there are 3D displacement components called U , V and W . θ is the twist angle.

Based on the assumption of small displacements and Vlasov's thin-walled beam theory for non-uniform torsion, Asgarian *et al.*, 2013 [5] derived a homogeneous fourth order differential equation with variable coefficients in terms of twist angle (θ), the bending moment (M_y) and section properties by uncoupling the system of differential equations governing the lateral-torsional stability behavior of tapered beams with thin-walled cross-sections. The resulting governing equilibrium equation in the case of singly symmetric compact cross-section is reduced to the following ones:

$$\begin{aligned} & \left[EI_{\omega} \theta'''' \right] - [GJ \theta'] - 2M_y' z_c' \theta - M_y z_c'' \theta - M_y'' z_c \theta \\ & - \frac{M_y^2}{EI_z} \theta + [\beta_z M_y \theta'] = -M_t \theta \end{aligned} \quad (1)$$

In the above-mentioned expression, the successive x -derivatives are denoted by $()'$, $()''$. In this equation, J and I_z signify the Saint-Venant torsion constant and the second moment of inertia, respectively. I_{ω} is the modified warping constant. Numerical formulations for computing these parameters relating to considered open section shapes in this study viz: doubly symmetric I section, singly symmetric I section and Tee section are presented in Appendix A. In the differential equation, M_t expresses the second order torsion moment due to load eccentricity ($M_t = q_z (z_p - z_c)$). β_z also illustrates Wagner's coefficient in which the exact formulation of this parameter is presented in [5].

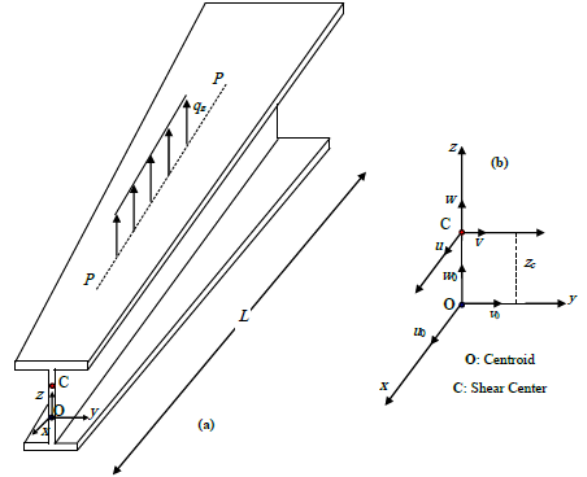


Fig. 1: (a) A tapered thin-walled beam with a singly symmetric I-section, (b) Coordinate system and notation of displacement parameters.

Extending the first equation results in:

$$\begin{aligned} & EI_{\omega} \frac{d^4 \theta}{dx^4} + 2E \frac{dI_{\omega}}{dx} \frac{d^3 \theta}{dx^3} \\ & + \left(E \frac{d^2 I_{\omega}}{dx^2} - GJ(x) + \beta_z M_y \right) \frac{d^2 \theta}{dx^2} \\ & + \left(\beta_z \frac{dM_y}{dx} + M_y \frac{d\beta_z}{dx} - G \frac{dJ}{dx} \right) \frac{d\theta}{dx} \\ & - (2M_y' z_c' + M_y z_c'' + M_y'' z_c + \frac{M_y^2}{EI_z} - M_t) \theta(x) = 0 \end{aligned} \quad (2)$$

For tapered thin-walled beams with singly-symmetric cross-section, the lateral-torsional stability analysis becomes more complex due to the presence of variable coefficients in the governing fourth order differential equation. Regarding this, the solution of the differential equation (2) is not straightforward and only numerical procedures such as Galerkin and Rayleigh-Ritz methods, differential transformation method, the power series expansions, finite difference method (FDM) and differential quadrature method (DQM) are possible. In the following, in order to solve the equilibrium equation (2) of non-prismatic thin-walled beams with singly-symmetric cross-section, the finite difference method is adopted. In order to solve the governing differential equation (Eq. (1)) based on this mathematical procedure, prescribed

boundary conditions including natural or geometrical ones at the two ends of the problem domain are required. It is noteworthy that the governing differential equation (Eq. (1)) is known as the strong form of the problem. Besides, to acquire the corresponding boundary conditions, the homogeneous differential equation should be transformed to a weighted-integral expression called the weak form which is equivalent to equilibrium equation and its relating boundary conditions. In order to construct the weak form for the governing differential equation, we should multiply Eq. (1) by an arbitrary function (ψ) and integrate the result over the problem domain. The weak form of the equilibrium equation in terms of the twist angle (Eq. (1)) is thus obtained by:

$$\int_0^L \psi \left((EI_{\omega} \theta'')'' - (GJ \theta')' - (M_y z_c)'' \theta \right) dx = 0 \quad (3)$$

$$\left(-\frac{M_y^2}{EI_z} \theta + (\beta_z M_y \theta')' + M_t \theta \right)$$

in which ψ is a test function which is continuous and satisfies the essential end conditions. Thus, the weak form for the equilibrium equation becomes:

$$\int_0^L \left((EI_{\omega} \theta'') \psi'' + GJ \theta' \psi' - (M_y z_c)'' \theta \psi \right) dx$$

$$\left(-\frac{M_y^2}{EI_z} \theta \psi - \beta_z M_y \theta' \psi' + M_t \theta \psi \right)$$

$$+ \left((EI_{\omega} \theta'')' - (GJ \theta') + (\beta_z M_y \theta') \right) \psi \Big|_0^L$$

$$- (EI_{\omega} \theta'') \psi' \Big|_0^L = 0 \quad (4)$$

In the current study, simply supported beams and cantilevers are surveyed. Their corresponding boundary conditions are thus defined as follows:

$$\text{Pinned support: } \theta = 0 \quad \text{and} \quad \frac{d^2 \theta}{dx^2} = 0 \quad (5)$$

$$\text{Clamped support: } \theta = 0 \quad \text{and} \quad \frac{d \theta}{dx} = 0 \quad (6)$$

$$\text{Free end: } \frac{d^2 \theta}{dx^2} = 0 \quad \text{and} \quad \frac{d}{dx} (EI_{\omega} \frac{d^2 \theta}{dx^2})$$

$$- (GJ - \beta_z M_y) \frac{d \theta}{dx} = 0 \quad (7)$$

3. FDM formulation of the problem

For solving differential equations with generalized end conditions, finite difference method is supposed to be a dominant numerical technique. Finite difference approach is a numerical iterative procedure that involves the use of successive approximations to obtain solutions of differential equations especially with variable coefficients. This numerical method is based on replacing each derivative in the differential equation (2), as well as its related boundary conditions (5-7) with finite difference formulations.

In order to apply the finite difference method to the equilibrium equation (2), the beam member with length of L is assumed to be sub-divided into n parts, with length

$h=L/n$, as shown in Fig. 2. Therefore, there are $(n+1)$ nodes along the beam's length with number $i=0, 1, \dots, n$, with 0 and n denoting beam ends. From numerical point of view, the second order forward difference formulation is used for the first-node ($i=0$) whereas for the last ($i=n$), the second order backward formulation is applied to the governing equation. For all the other nodes ($0 < i < n$), the second order central difference formulation is implemented.

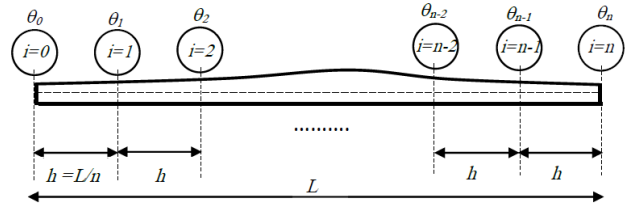


Fig. 2: Finite Difference Method: Definition spaced grid points.

The finite difference form of the governing differential equation at node i , can be expressed as follow:

$$EhI_{\omega}^L (\theta_{i+2} - 2\theta_{i+1} + 2\theta_{i-1} - \theta_{i-2}) + Eh^2 I_{\omega}^m (\theta_{i+1} - 2\theta_i + \theta_{i-1})$$

$$+ EI_{\omega}^- (\theta_{i+2} - 4\theta_{i+1} + 6\theta_i - 4\theta_{i-1} + \theta_{i-2})$$

$$- Gh^2 J_i (\theta_{i+1} - 2\theta_i + \theta_{i-1}) - \frac{h^3}{2} GJ_i' (\theta_{i+1} - \theta_{i-1})$$

$$- 2h^4 M_{yi}^{\prime} z_{ci}^{\prime} \theta_i - h^4 M_{yi} z_{ci}^{\prime \prime} \theta_i - h^4 M_{yi}^{\prime \prime} z_{ci} \theta_i - h^4 \frac{M_{yi}^2}{EI_{zi}} \theta_i$$

$$+ \frac{h^3}{2} (\beta_{zi}^{\prime} M_{yi} + \beta_{zi} M_{yi}^{\prime}) (\theta_{i+1} - \theta_{i-1})$$

$$+ h^2 (\beta_{zi} M_{yi}) (\theta_{i+1} - 2\theta_i + \theta_{i-1}) + M_{ti} \theta_i = 0 \quad (8)$$

Or

$$+ \theta_{i-2} (EI_{\omega}^- - EhI_{\omega}^L)$$

$$+ \theta_{i-1} \left(2EhI_{\omega}^L + Eh^2 I_{\omega}^m - 4EI_{\omega}^- - Gh^2 J_i \right.$$

$$\left. + 0.5h^3 GJ_i' - 0.5h^3 (\beta_{zi} M_{yi})' + h^2 (\beta_{zi} M_{yi}) \right)$$

$$+ \theta_i \left(6EI_{\omega}^- - 2Eh^2 I_{\omega}^m + 2Gh^2 J_i - 2h^4 M_{yi}^{\prime} z_{ci}^{\prime} \right.$$

$$\left. - h^4 M_{yi} z_{ci}^{\prime \prime} - h^4 M_{yi}^{\prime \prime} z_{ci} - h^4 \frac{M_{yi}^2}{EI_{zi}} \right.$$

$$\left. - 2h^2 (\beta_{zi} M_{yi}) - M_{ti} \right)$$

$$+ \theta_{i+1} \left(Eh^2 I_{\omega}^m - 2EhI_{\omega}^L - 4EI_{\omega}^- - Gh^2 J_i \right.$$

$$\left. - 0.5h^3 GJ_i' + 0.5h^3 (\beta_{zi} M_{yi})' + h^2 (\beta_{zi} M_{yi}) \right)$$

$$\theta_{i+2} (EhI_{\omega}^L + EI_{\omega}^-) = 0 \quad (9)$$

in which, $\theta_{i-2}, \theta_{i-1}, \theta_i, \theta_{i+1}$ and θ_{i+2} are the angle of twist of the considered member in five points, located at equal distances of h .

In the following, Eq. (9) should be written for $n-1$ grid points of a divided element. $(n-1)$ equations are thus derived including $n+3$ unknown parameters ($\theta_{-1}, \theta_0, \theta_1, \dots, \theta_n, \theta_{n+1}$). In order to solve the system of obtained equations by the finite difference method, four equations eventuated from boundary conditions of the beam are required as follows:

- Simply supported beams:

$$\begin{aligned}
 i = 0 & \rightarrow \begin{cases} \theta_0 = 0 \\ 2\theta_0 - 5\theta_1 + 4\theta_2 - \theta_3 = 0 \end{cases} \\
 i = n & \rightarrow \begin{cases} \theta_n = 0 \\ 2\theta_n - 5\theta_{n-1} + 4\theta_{n-2} - \theta_{n-3} = 0 \end{cases}
 \end{aligned} \quad (10)$$

- Cantilever beams:

$$\begin{aligned}
 i = 0 & \rightarrow \begin{cases} \theta_0 = 0 \\ -3\theta_0 + 4\theta_1 - \theta_2 = 0 \end{cases} \\
 i = n & \rightarrow \begin{cases} 2\theta_n - 5\theta_{n-1} + 4\theta_{n-2} - \theta_{n-3} = 0 \\ EI_{\bar{\omega}} \begin{pmatrix} 2.5\theta_n - 9\theta_{n-1} + 12\theta_{n-2} \\ -7\theta_{n-3} + 1.5\theta_{n-4} \end{pmatrix} \\ -h^2(GJ - \beta_z M_y)(1.5\theta_n - 2\theta_{n-1} + 0.5\theta_{n-2}) = 0 \end{cases}
 \end{aligned} \quad (11)$$

It is worth mentioning that forward and backward finite difference formulations are respectively implemented for the first ($i=0$) and last ($i=n$) nodes. In this manner, no virtual nodes are required and the overall error is thus reduced. Therefore, finite difference approach in the presence of n equal segments constitutes a system of simultaneous equations with $(n+3)$ linear equations. In the following, the simplified equilibrium equation through FD formulation is written in a matrix notation as follows:

$$([R] + [R^*])\{\theta\}_{n+3 \times 1} = \{0\}_{n+3 \times 1} \quad (12)$$

R and R^* are $n+3 \times n+3$ matrices. As previously mentioned, n denotes the number of segments along the computation domain ($0 \leq x \leq L$). Regarding Eq. (9), the terms of R and R^* for $1 \leq i \leq n-1$ are determined in the following forms:

$$\begin{aligned}
 R_{i,i} &= EI_{\bar{\omega}}' - EhI_{\bar{\omega}}', \\
 R_{i,i+1} &= 2EhI_{\bar{\omega}}' + Eh^2I_{\bar{\omega}}'' - 4EI_{\bar{\omega}}' - Gh^2J_i + \frac{h^3}{2}GJ_i', \\
 R_{i,i+2} &= 6EI_{\bar{\omega}}' - 2Eh^2I_{\bar{\omega}}'' + 2Gh^2J_i, \\
 R_{i,i+3} &= Eh^2I_{\bar{\omega}}'' - 2EhI_{\bar{\omega}}' - 4EI_{\bar{\omega}}' - Gh^2J_i - \frac{h^3}{2}GJ_i', \\
 R_{i,i+4} &= EhI_{\bar{\omega}}' + EI_{\bar{\omega}}', \\
 R_{i,i+1}^* &= -0.5h^3(\beta_{zi}M_{yi})' + h^2(\beta_{zi}M_{yi}), \\
 R_{i,i+2}^* &= -2h^4M_{yi}'z_{ci}' - h^4M_{yi}z_{ci}'' - h^4M_{yi}''z_{ci} \\
 &\quad - h^4\frac{M_{yi}^2}{EI_{zi}} - 2h^2(\beta_{zi}M_{yi}) - M_{ti}, \\
 R_{i,i+3}^* &= 0.5h^3(\beta_{zi}M_{yi})' + h^2(\beta_{zi}M_{yi}).
 \end{aligned} \quad (13a, h)$$

In Eq. (12), $\{\theta\}$ is the displacement vector:

$$\{\theta\}^T = \{\theta_{-1} \ \theta_0 \ \theta_1 \ \theta_2 \ \dots \ \theta_{n-1} \ \theta_n \ \theta_{n+1}\} \quad (14)$$

The remaining constants in matrices $[R]$ and $[R^*]$ are obtained from the boundary conditions:

- Simply supported beams:

$$\begin{cases} R_{n,2} = 1, \\ R_{n+1,2} = 2, R_{n+1,3} = -5, R_{n+1,4} = 4, R_{n+1,5} = -1 \\ R_{n+2,n+2} = 1, \\ R_{n+3,n+2} = 2, R_{n+3,n+1} = -5, R_{n+3,n} = 4, R_{n+3,n-1} = -1 \end{cases} \quad (16)$$

- Cantilever beams:

$$\begin{cases} R_{n,2} = 1, \\ R_{n+1,2} = -3, R_{n+1,3} = 4, R_{n+1,4} = -1 \\ R_{n+2,n+2} = 2, R_{n+2,n+1} = -5, R_{n+2,n} = 4, R_{n+2,n-1} = -1 \\ R_{n+3,n+2} = 2.5EI_{\bar{\omega}} - 1.5h^2(GJ - \beta_z M_y), \\ R_{n+3,n+1} = -9EI_{\bar{\omega}} + 2h^2(GJ - \beta_z M_y), \\ R_{n+3,n} = 12EI_{\bar{\omega}} - 0.5h^2(GJ - \beta_z M_y), \\ R_{n+3,n-1} = -7EI_{\bar{\omega}}, R_{n+3,n-2} = 1.5EI_{\bar{\omega}} \end{cases}$$

System (12) is fulfilled with the condition that the determinant of the matrix $([R] + [R^*])$ be zero. The smallest positive real root of the equation is considered as critical buckling load. The critical buckling load will be close to the exact value by increasing the number of segments. In the following, the finite difference method is applied to study the stability analysis of thin-walled beams with different boundary conditions and arbitrary loadings, in the presence of variable cross-sections. The critical buckling load is calculated by using eigenvalue. The calculation procedure is done with the aid of MATLAB software [22].

4. Numerical Examples

By means of two selected numerical examples, the efficiency, accuracy and precision of the finite difference method in lateral-torsional buckling analysis of tapered thin-walled beams with singly-symmetric cross-section are studied below. The results are compared to other analytical and numerical solutions presented in literature, as well as finite element method by means of ANSYS [4].

4-1 Example 1- Simply supported web-tapered beam under gradient moment:

This example investigates the lateral buckling stability of a simply supported tapered beam under gradient moments ($M_0, \psi M_0$) applied at supports (Fig.3a). The gradient moment factor (ψ) varies from +1 to -1. In this study, the beam length is $L=9$ m. The beam has three different cross-sections at the first support depicted in (Fig. 3 b, c, d). The first two sections are doubly and singly symmetric I section and the third one is a Tee section. The cross section height decreases from h_{max} at the left support to $h_{min} = \alpha h_{max}$ at the right one.

The elastic lateral-torsional buckling moments are evaluated for different values of gradient moment ψ ($-1 \leq \psi \leq 1$) and tapering coefficient α (0.4, 1). The material data is depicted in Fig. 3. According to the loading condition and Fig. 3, the expression for the bending variation M_y is equal to:

$$M_y(x) = M_0 \left(1 - \frac{x}{L}\right) + \psi M_0 \frac{x}{L} \quad (17)$$

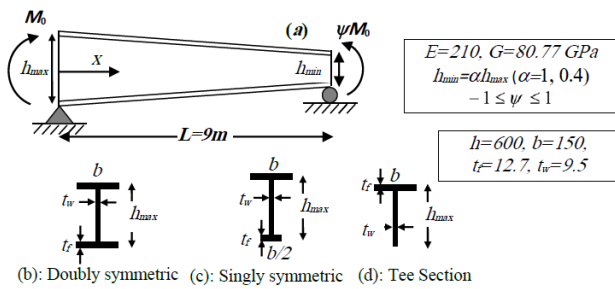


Fig. 3 - Simply supported tapered beam under moment gradient: (a): geometry and material properties, (b) doubly symmetric section, (c) singly symmetric section and (d) Tee section.

Taking into account the author's knowledge on PSM [5], the results of this numerical approach are very sensitive to the number of terms considered in the power series approximations. Therefore, in each case of loading, it is important to estimate the needed number of terms of power series to evaluate an explicit expression for deformation shape of the member and then to calculate the lowest lateral-torsional buckling loads below an acceptable relative error. According to [5], for most of the external bending load cases, it is not indispensable to use more than 20 terms in power series expansions, in order to obtain critical elastic buckling loads with exceptionally good accuracy. But in the case of negative gradient moment loading ($-1 \leq \psi < 0$) and according to Eq. (17), the sign for bending moment changes from positive to negative. Therefore, predicting the exact deformation of the buckling mode of the beam under mentioned external loading condition is significantly complicated due to the concavity changes. One can check that the lateral buckling modes are highly dependent on the cross section shape and gradient moments. They are available in [23]. For this reason, the solution of fourth-order differential equation (1) becomes absolutely difficult when the gradient factor (ψ) is negative. It can be concluded that for equivalent accuracy of lateral-buckling loads of members under variable negative bending moment, and specifically for a non-uniform beam with non-symmetric cross-section under these circumstances, it is obviously required to consider more than 20 terms of power series to determine a more accurate deformation shape. In this regard, in the first stage of the current example, the lateral buckling moment of the prismatic and tapered beam with singly symmetric I section under a negative gradient moment ($M_0, -0.5M_0$) needs to be contemplated to estimate the required numbers of terms of power series and finite difference approach. Therefore, the first two buckling loads are researched according to the number of divisions in FDM and the number of terms of power series in PSM needed for convergence which are illustrated in Table 1. The results are compared to FEM simulations. In this

example, the studied homogeneous thin-walled beam has been modeled using shell elements (SHELL63) of Ansys code. Shell63 has both bending and membrane capabilities. Both in-plane and normal loads are also permitted. The element has 6 degrees of freedom at each node, 3 translations in x, y and z directions and 3 rotations about the 3 axes. In this paper, for all developed models by Ansys, the adopted aspect ratio of the element (length-to-maximum width) was close to unity at the largest cross-section. The first two lateral-torsional buckling mode shapes of the prismatic and tapered beams with mono-symmetric I-section under ($M_0, -0.5M_0$) are represented in Fig. 4.

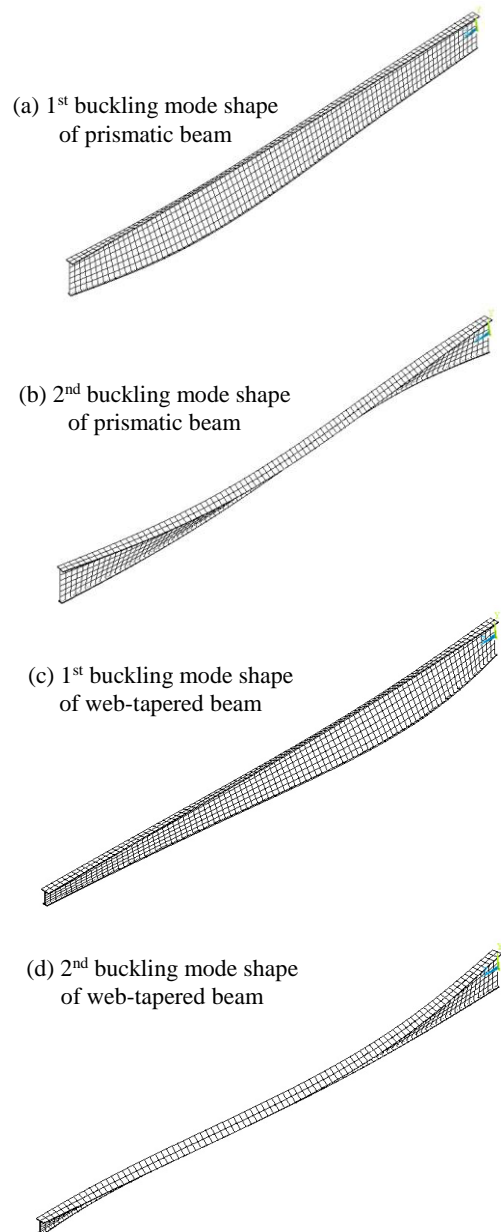


Fig. 4: The uniform shell mesh used for beam with singly symmetric I-section subjected to gradient moment ($M_0, -0.5M_0$).

Table 1: Effect of number of divisions (FDM) and power series terms (PSM) on linear critical moments (M_{cr}) of simply supported thin-walled beam with mono-symmetric cross-section under ($M_0, -0.5M_0$). Buckling moments and CPU time comparisons.

Beam Type	Mode	The critical bending moments ($kN.m$), accompanied with the average CPU time (s)										
		Proposed FDM					PSM					ANSYS
		Number of divisions					Number of terms of power series					
		10	15	20	30	40	50	30	40	50	60	
Prismatic Beam	1	89.765 (5.30s)	85.561 (7.91s)	84.103 (10.83s)	83.032 (19.63s)	82.665 (25.67s)	82.495 (41.29s)	70.35 (12.21s)	79.46 (60.61s)	80.74 (1437.70s)	80.75 (3075.90s)	82.19 (22.5s)
	2	204.216	195.415	192.346	190.174	189.395	189.030	291.3	200.08	191.36	190.45	188.4
Tapered Beam ($\alpha=0.4$)	1	88.248 (5.68s)	83.658 (8.17)	82.088 (11.41s)	80.984 (20.05s)	80.595 (26.05s)	80.411 (40.36s)	62.56 (12.61s)	69.87 (131.50s)	74.81 (3989.02s)	76.92 (13244.5s)	80.09 (26.2s)
	2	198.020	190.997	188.650	186.915	186.287	186.005	303.05	221.73	195.42	192.63	185.51

4.1.1. Comparison of FDM and PSM results

As can be seen in Table 1, the satisfactory results for engineering requirements can be reached by discretizing the beam's length into 30 segments according to the FDM formulation investigated in the current paper. With the help of PSM, one needs more than 50 terms to achieve the same accuracy. Moreover, the elapsed time to perform numerical computations is presented in Table 1. Table 1 shows that Central Processing Unit (CPU) needs an average of 19.63 seconds to accomplish FDM simulation for a prismatic beam with 30 divisions. The buckling moment is 83.032 kN.m (error $\Delta=1\%$). When the number of divisions is increased to 50, the buckling moment is close to shell results ($M_{cr}=82.495 \text{ kN.m}$, error $\Delta<0.5\%$). The needed CPU time is only 41.29s. With the PSM, an accurate value of buckling moment equal to 79.46 kN.m (error $\Delta=3\%$) is obtained with a number terms in the series equaling to 40. This method requires 60.61 s CPU time. In order to improve the results, more CPU times are needed. With 50 terms the buckling moment is 80.74 kN.m (error $\Delta=2\%$) and the CPU time is impressive (1437 s). When the number terms is increased, the buckling moment becomes insensitive and the CPU time increases accordingly. Additionally, for this example the relative error of FDM is less than its counterpart in PSM. This proves that PSM could be effectively replaced by FDM in this example. The same statement is true for non-prismatic beam in Table 1.

Note that according to the FDM, boundary conditions and arbitrary loads and cross section shapes have no special influences on the results and for most of the studied cases. For this reason, in the following examples, the beam is divided into 30 segments.

The main gist of the load case depicted in Fig.3a relating to three different considered cross-sections, as shown in Fig. 3b-d, are commented below. Before expressing the conclusions of this example, it should be pointed out that the outcomes are valid only for the cross-sections studied.

4.1.2. Lateral buckling strength of simply supported beam with doubly symmetric cross section

The buckling moment variations in terms of the gradient moment are depicted in Fig. 5. The lateral buckling

strengths of the prismatic beam with doubly symmetric I section are presented in Fig. 5a. It can be concluded that there is an excellent agreement between the buckling moments calculated by proposed numerical formulation and those estimated by finite element simulations, using shell element of ANSYS software [4]. The relative difference between the two abovementioned methods is about 1%.

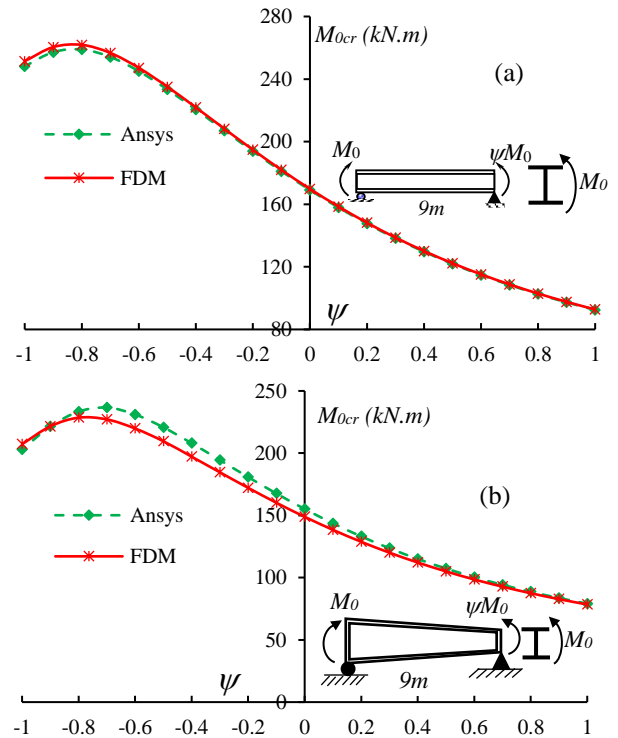


Fig. 5: Variation of lateral buckling moment of beam with doubly-symmetric I-section under gradient moment, versus the gradient factor ψ . (a) prismatic beam, (b) tapered beam.

The variation of lateral buckling moments of the simply supported web tapered beam with doubly symmetric I-section subjected to gradient bending moment versus the gradient coefficient (ψ) is also represented in Fig. 5b. As can be seen, the results of the present method (FDM) and ANSYS code are very close especially for positive

gradient factor ($0 \leq \psi \leq 1$). Under negative factor, critical moments computed from FDM underestimate tapered beam strength (3% error). According to Fig. 5a, b and for both uniform and non-uniform beams with doubly symmetric cross-section under bending moment, variation of the lateral buckling resistance is non-linear with ψ . Besides, the maximum strength is reached when $\psi = -0.8$ for the prismatic beam. These results are confirmed in [23]. In the case of the tapered beam the maximum strength is obtained for $\psi = -0.7$. This result is original.

4.1.3. Lateral buckling strength of simply supported beam with singly symmetric cross section

In the case of mono-symmetric I-section, the lowest two buckling moments variation versus the gradient moment factor for prismatic and non-prismatic beams are respectively presented in Figs. 6 and 7. In the case of the lowest critical buckling moment corresponding to the first mode, it is supposed that the bottom flange, precisely the shorter one is in compression and those related to the second mode are evaluated when gradient moment loading causes compressive stress on the top flange (the longer one) of mono-symmetric I-section.

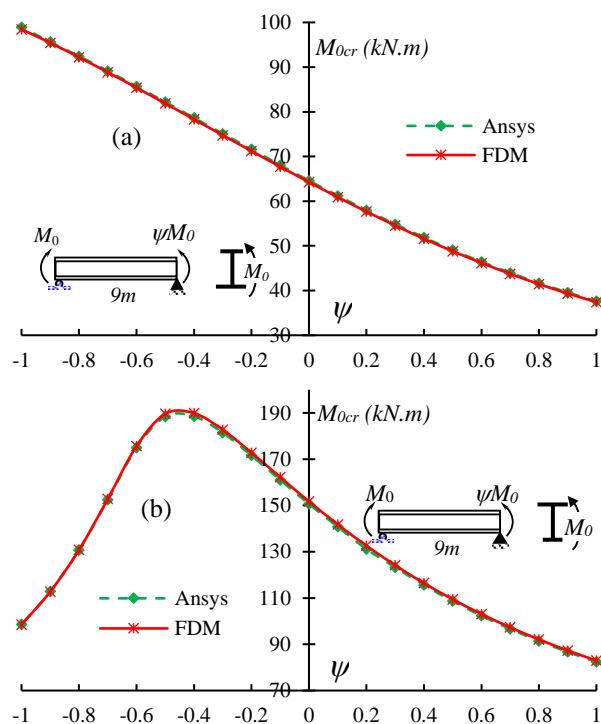


Fig. 6: Variation of lateral buckling moment of prismatic beam with mono-symmetric I-section under gradient moment, versus gradient factor ψ : (a) largest flange in tension under (M_0), (b) largest flange in compression under (M_0).

In the case of the prismatic beam with mono-symmetric section, the strength of the beam under gradient moment, which depends on cross-section deformation, is pictured in Fig. 6. One can remark that when the largest flange is in tension under M_0 , the variation of the beam strength with gradient coefficient (ψ) is linear and the highest and lowest resistances are acquired under $\psi = -1$ and $\psi = 1$, respectively. When the largest flange is in

compression under M_0 (Fig. 6b), non-linear variation of lateral buckling resistance of beam with (ψ) is noticed. The highest strength is also obtained near $\psi = -0.5$. These results are in good agreement with Mohri *et al.*, 2013 [23].

For the tapered thin-walled beam with mono-symmetric section, the negative and positive lateral buckling moments variations with ψ are depicted in Fig. 7a, b. Under positive and negative gradient moments (Fig. 7), the outcomes of proposed finite difference method concord very well with ANSYS simulations. It should be noted that the great strength of tapered thin-walled beam with mono-symmetric I-section is obtained under positive gradient moment. The highest strength is also obtained near $\psi = -0.5$. These results are original and have never studied before.

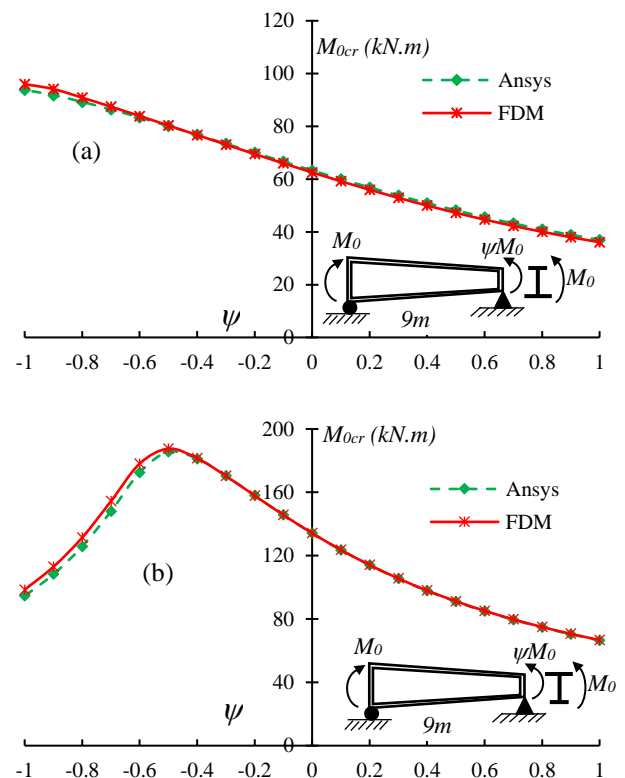


Fig. 7: Variation of lateral buckling moment of non-prismatic beam with mono-symmetric I-section under gradient moment, versus gradient factor ψ : (a) largest flange in tension under (M_0), (b) largest flange in compression under (M_0).

4.1.4. Lateral buckling strength of simply supported beam with Tee section

For this cross section, the lowest two buckling moments variation versus the gradient moment factor for the prismatic and tapered beams are depicted in Figs. 8 and 9, respectively. In the case of positive moment loading, it is supposed that the flange of Tee section is under compression; nevertheless, negative moment loading causes tension stress on the flange of Tee section. It is observed again that the strength of the beam under gradient moment depends strongly on cross-section deformation either in the case of the prismatic beam and the tapered one (Figs. 8, 9). It should be noted that the great resistance of the thin walled beam with Tee section under a gradient

moment (M_0 , ψM_0) is acquired when flange of section is in compression under bending moment.

In the case of thin-walled beam with constant Tee section, when the flange is in tension under M_0 (Fig. 8a), the variation of the beam strength with gradient coefficient (ψ) is linear and the highest and lowest resistances are acquired under $\psi=-1$ and $\psi=1$, respectively. When the flange is in compression under M_0 (Fig. 8b), non-linear variation of lateral buckling resistance of beam with (ψ) is observed. The highest strength is obtained near $\psi=-0.3$. These results are in good agreement with Mohri *et al.*, 2013 [23].

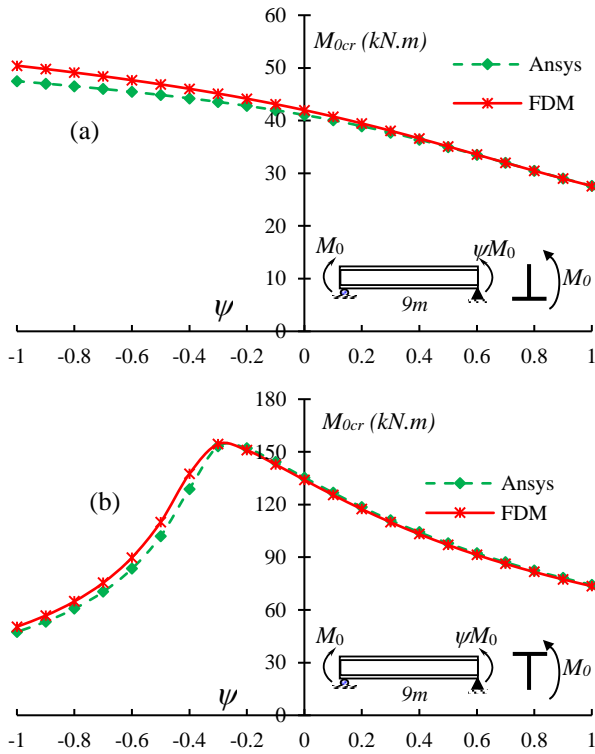


Fig. 8: Variation of lateral buckling moment of prismatic beam with Tee section under gradient moment, versus gradient factor ψ : (a) flange in tension under (M_0), (b) flange in compression under (M_0).

For the tapered thin-walled beam, the positive and negative lateral buckling moments variations with ψ are depicted in Fig. 9a, b. When gradient factor is positive ($\psi > 0$), buckling results derived from finite difference approach are in good agreement with ANSYS software predictions, but when gradient coefficient is negative ($\psi < 0$), lateral buckling moments obtained by present numerical method overestimate beam resistance (6% error). It should be noted that the great strength of tapered thin-walled beam with mono-symmetric I-section is obtained under positive gradient moment. The highest strength is also obtained near $\psi=-0.4$. These results are original and have never been studied before.

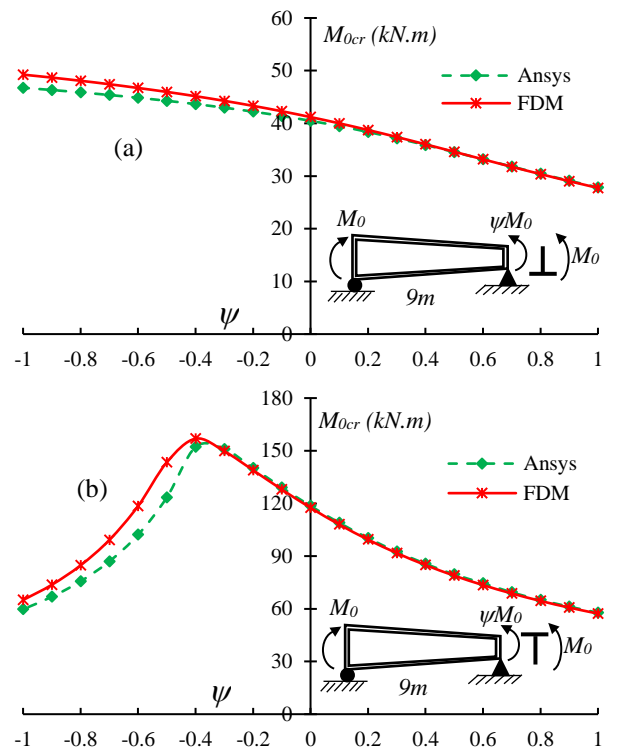


Fig. 9: Variation of lateral buckling moment of tapered beam with Tee section under gradient moment, versus gradient factor ψ : (a) flange in tension under (M_0), (b) flange in compression under (M_0).

4-2 Example 2- Cantilever web and flanges tapered beam under uniformly distributed load:

This section deals with the stability analysis of three sets of cantilever non-prismatic thin-walled beams subjected to a distributed load. The linear lateral buckling loads of the beams are carried out with the presence of doubly or singly symmetric I-cross-sections and also Tee section. In the illustrated member, the geometrical properties of the clamped end section of the beam are constant; nevertheless, the flanges' width and the web height for all considered types of cross-sections are made to vary linearly from the fixed end to the free one. The geometrical data for the stipulated beams are shown in Fig. 10.

In the case of doubly symmetric I-section, the linear lateral buckling loads are derived for two load positions: load on the centroid and the top flange. The stability analysis is made for a singly symmetric I-section when the lateral distributed load is applied at two different positions: the top flange and the bottom one. The critical buckling loads for the considered member with Tee section are also computed when uniformly distributed load is applied on the top flange. Buckling analysis is carried out for different beam lengths $L=6$ to 12m. For this example, shear and Young's modulus of material for all considered thin-walled beams are taken as $G=80.77\text{GPa}$ and $E=210\text{GPa}$, respectively.

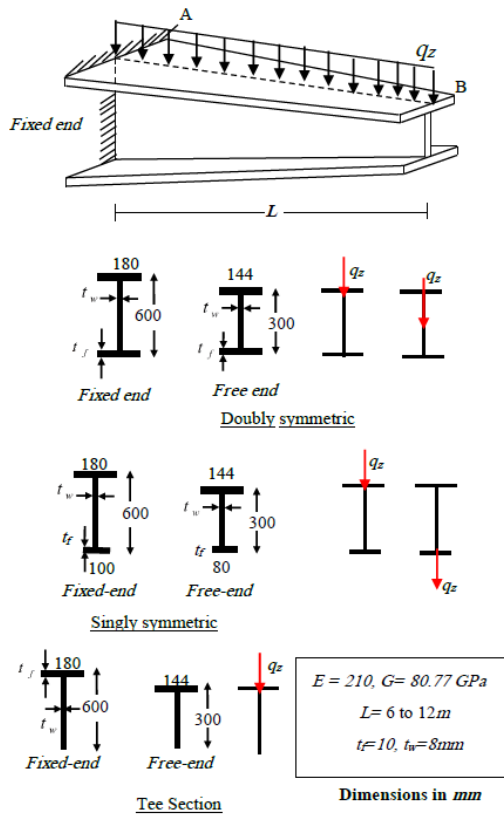


Fig. 10: Cantilever web tapered beam with doubly or singly symmetric I-section and Tee section: geometry, material and loading properties.

The variation of linear critical buckling loads of the cantilever thin-wall beams under lateral distributed load with different beam lengths for above mentioned three types of cross-sections are illustrated in Figs. 11 to 13. For more comparisons, the same figures show the results obtained by finite element using ANSYS software. According to the above figures, it can be concluded that finite difference solutions overestimate the lateral critical buckling loads. However, in the case of short beam ($L=6$ m), the significant differences between shell predictions of ANSYS and the obtained results by proposed numerical method are conspicuous. For this case, the effects of the distortion, local buckling deformation and local influences of lateral load are evident in the overall buckling results of shell modeling. None of the mentioned phenomena is considered in the formulation of the proposed technique based on beam theory. As illustrated in Figs. 11 to 13, in the case of long beams ($L=11$ and 12 m), the ANSYS results and proposed FDM are very close. In these cases, slender beams are obtained, so most of the abovementioned problems can be reduced consequently.

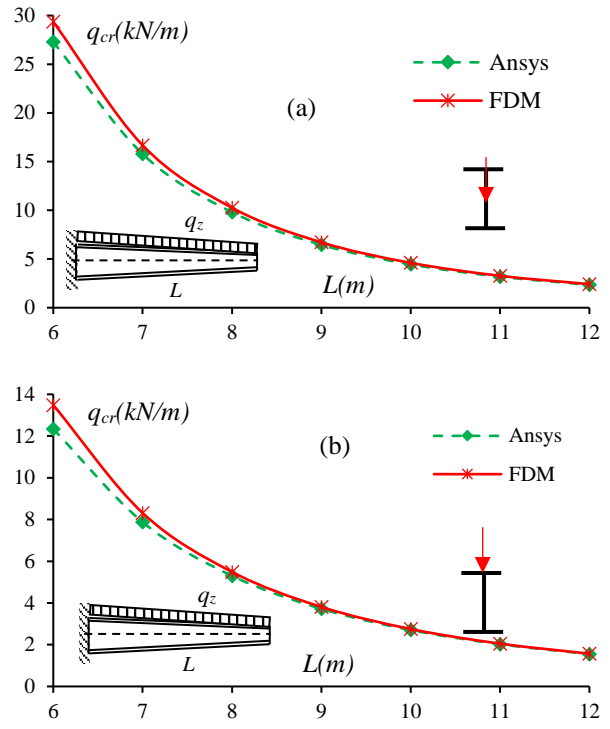


Fig. 11: Lateral Buckling loads variation versus length L of the tapered beam with doubly symmetric cross section, (a): centroid loading, (b): top flange loading.

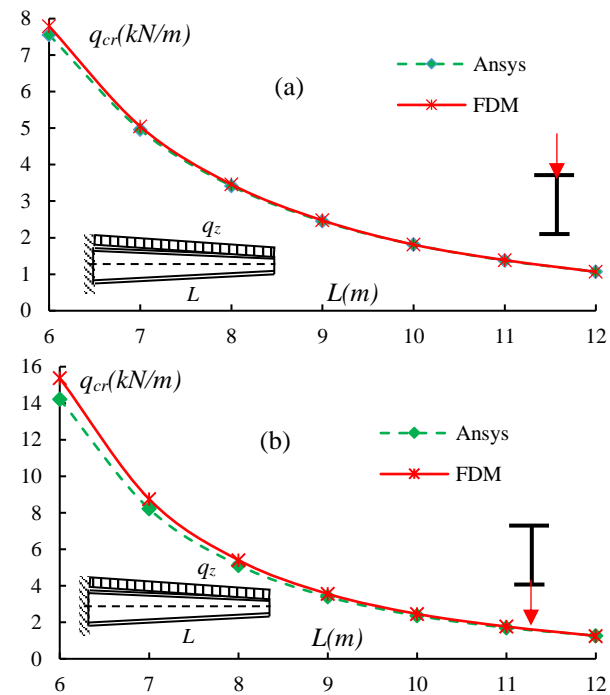


Fig. 12: Lateral Buckling loads variation versus length L of the tapered beam with singly symmetric cross section, (a): top flange loading, (b): bottom flange loading.

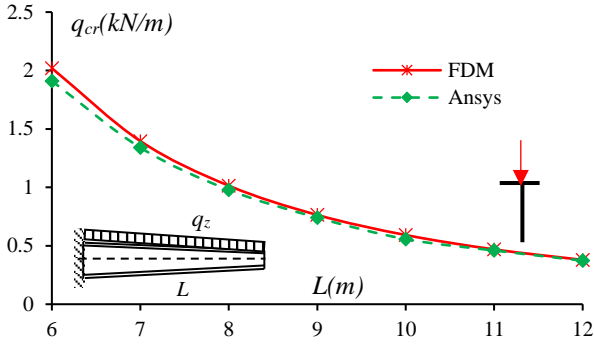


Fig. 13: Critical buckling loads variation versus length L of the Tapered beam with Tee cross section (load on top flange).

5. Conclusions

In the present study, the linear stability analysis of elastic tapered thin-walled beam under arbitrary bending loads has been investigated using finite difference approach. In the presence of arbitrary variation in cross-section and external loads, the governing equilibrium equation becomes a differential equation with variable coefficients in which the classical methods used in stability analysis of prismatic members are not efficient and no longer valid. The finite difference method is thus adopted to solve the fourth-order differential equation with variable coefficients of non-prismatic beams with general boundary conditions. Finally, the critical buckling loads are obtained by solving the eigenvalue problem resulting from a system of equations obtained from FDM.

In order to demonstrate the accuracy and efficiency of the FDM, two examples have been considered. Beams with different boundary conditions and arbitrary bending loads are studied. Effects of end conditions, loading position, beam's length, tapering and cross-section shape have also been investigated. The results of the present method have been compared to ANSYS code simulations or other results available in the literature. In most cases, it could be concluded that by discretizing the considered member into 30-40 divisions the critical buckling loads of non-uniform members can be determined with a very good accuracy. The FDM is more efficient in the presence of tapering and non-symmetric buckling modes. In some complicated cases, this method is more accurate than the PSM and requires less CPU times. Nevertheless, there are some cases in which PSM is more accurate than FDM. The results of the current study prove that the CPU time is a concern in PSM method, suggesting that using a hybrid method, which is a combination of FDM and PSM, can be a valuable alternative.

Appendix A

In this appendix, exact formulations for computation of the geometrical characteristics of an open thin-walled section, such as I_z , J , z_c and I_{ω} are presented. In [5], the absolute formulations of these parameters are expressed. The characteristics of any geometrical properties of the beam are a function of the coordinate x due to the tapering of the web and/or flanges. In this study, it is assumed that the thickness of the web (t_w) and flanges (t_f) are constant over

the length of the beam. In the following, the geometrical parameters at the left support ($x=0$) and the right one ($x=L$) of the beam are respectively indicated with the subscripts 0 and 1. In the present study, doubly symmetric I section, singly symmetric I section and Tee section, as shown in Fig. A1, are surveyed.

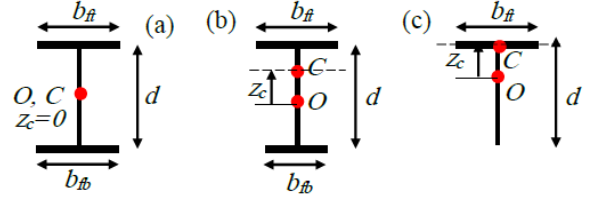


Fig. A1: (a) doubly symmetric I section, (b) singly symmetric I section, (c) Tee section.

In the case of doubly symmetric I section, the width of both the top and bottom flanges are equal ($b_{ft}=b_{fb}=b_f$). For Tee section, the width of bottom flange is zero ($b_{fb}=0$). It should be pointed out that d signifies the height for I sections, measured between the flange mid-lines.

In the case of web tapered, the height of the beam's section is (d_0) at the left support and is linearly changed to ($d_1 = \alpha d_0$) at the other end. The expression describing web linear variation is thus defined as:

$$h_w = d_0(\alpha - 1)\left(\frac{x}{L}\right) + d_0 \quad (\text{A.1})$$

In the case of the beam with tapered flanges, the width of the top and bottom are respectively made to vary linearly to $b_{ft1} = \beta_t b_{ft0}$ and $b_{fb1} = \beta_b b_{fb0}$ at the other end with different tapering ratios. Therefore, the variation of the top and bottom flanges can be respectively expressed as follows:

$$B_{fT} = b_{ft0}(\beta_t - 1)\left(\frac{x}{L}\right) + b_{ft0} \quad (\text{A.2})$$

$$B_{fb} = b_{fb0}(\beta_b - 1)\left(\frac{x}{L}\right) + b_{fb0} \quad (\text{A.3})$$

A.1. Expression of the second moment of inertia (I_z):

The expression of minor axis moment of inertia (I_z) about centroid is:

$$I_z = \int_A y^2 dA \quad (\text{A.4})$$

By performing integration over the cross-sectional area in the context of principal axes, this expression (I_z) for three different contemplated sections is reduced to the following ones:

- Doubly symmetric I section:

$$I_z = \frac{1}{6}t_f \left(b_{ft0}(\beta - 1)\left(\frac{x}{L}\right) + b_{ft0} \right)^3 + \frac{1}{12}t_w^3 \left(d_0(\alpha - 1)\left(\frac{x}{L}\right) + d_0 - t_f \right)^3 \quad (\text{A.5})$$

- Singly symmetric I section:

$$I_z = \frac{1}{12} t_f \left\{ \left(b_{ft0}(\beta_t - 1) \left(\frac{x}{L} \right) + b_{ft0} \right)^3 + \left(b_{fb0}(\beta_b - 1) \left(\frac{x}{L} \right) + b_{fb0} \right)^3 \right\} \quad (\text{A.6})$$

$$+ \frac{1}{12} t_w^3 \left(d_0(\alpha - 1) \left(\frac{x}{L} \right) + d_0 - t_f \right)$$

- Tee section:

$$I_z = \frac{1}{12} t_f \left(b_{ft0}(\beta_t - 1) \left(\frac{x}{L} \right) + b_{ft0} \right)^3 + \frac{1}{12} t_w^3 \left(d_0(\alpha - 1) \left(\frac{x}{L} \right) + d_0 - t_f \right) \quad (\text{A.7})$$

A.2. Expression of the Saint-Venant torsion constant (J):

The formulation of this coefficient is recalled here [5]:

$$J = \int_A \left(y - \frac{\partial \omega}{\partial z} \right)^2 + \left(z + \frac{\partial \omega}{\partial y} \right)^2 dA \quad (\text{A.8})$$

In the abovementioned formulation, the term $\omega(y, z)$ is the warping function, which can be defined based on Saint Venant's torsion theory. The Saint-Venant torsion constant for a thin-walled open section made from N straight segments can be thus obtained as:

$$J = \sum_{k=1}^N \frac{l_k t_k^3}{3} \quad (\text{A.9})$$

in which, l_k and t_k are length and thickness of each segment, respectively. Therefore, this parameter (J) for the three considered sections is:

- Doubly symmetric I section:

$$J = \frac{2}{3} t_f^3 \left(b_{f0}(\beta - 1) \left(\frac{x}{L} \right) + b_{f0} \right)^2 + \frac{1}{3} t_w^3 \left(d_0(\alpha - 1) \left(\frac{x}{L} \right) + d_0 - t_f \right) \quad (\text{A.10})$$

- Singly symmetric I section:

$$J = \frac{1}{3} t_f^3 \left\{ \left(b_{ft0}(\beta_t - 1) \left(\frac{x}{L} \right) + b_{ft0} \right)^2 + \left(b_{fb0}(\beta_b - 1) \left(\frac{x}{L} \right) + b_{fb0} \right)^2 \right\} \quad (\text{A.11})$$

$$+ \frac{1}{3} t_w^3 \left(d_0(\alpha - 1) \left(\frac{x}{L} \right) + d_0 - t_f \right)$$

- Tee section:

$$J = \frac{1}{3} t_f^3 \left(b_{ft0}(\beta_t - 1) \left(\frac{x}{L} \right) + b_{ft0} \right)^2 + \frac{1}{3} t_w^3 \left(d_0(\alpha - 1) \left(\frac{x}{L} \right) + d_0 - t_f \right) \quad (\text{A.12})$$

A.3. Expression of the position of shear center z_c :

The distance between the shear center and the centroid is denoted by z_c , which can be determined for each of considered open section with the following formulations:

- Doubly symmetric I section:

$$z_c = 0$$

- Singly symmetric I section:

$$A = t_f \left(b_{ft0}(\beta_t - 1) \left(\frac{x}{L} \right) + b_{ft0} \right) + t_w \left(b_{fb0}(\beta_b - 1) \left(\frac{x}{L} \right) + b_{fb0} \right) \quad (\text{A.13})$$

$$+ t_w \left(d_0(\alpha - 1) \left(\frac{x}{L} \right) + d_0 - t_f \right)$$

Then, one gets: (A.14)

$$z_c = \left(1 + \left(\frac{b_{ft0}(\beta_t - 1) \left(\frac{x}{L} \right) + b_{ft0}}{b_{fb0}(\beta_b - 1) \left(\frac{x}{L} \right) + b_{fb0}} \right)^3 \right)^{-1} \times \left(d_0(\alpha - 1) \left(\frac{x}{L} \right) + d_0 - t_f \right) - \frac{1}{A} \left\{ 0.5 t_f^2 \left(b_{ft0}(\beta_t - 1) \left(\frac{x}{L} \right) + b_{ft0} \right) + 0.5 t_w \left(d_0(\alpha - 1) \left(\frac{x}{L} \right) + d_0 - t_f \right) \left(d_0(\alpha - 1) \left(\frac{x}{L} \right) + d_0 + t_f \right) + t_f \left(b_{fb0}(\beta_b - 1) \left(\frac{x}{L} \right) + b_{fb0} \right) \left(d_0(\alpha - 1) \left(\frac{x}{L} \right) + d_0 + 0.5 t_f \right) \right\} - 0.5 t_f$$

A.4. Expression of the modified warping constant (I_{ω}):

The modified warping constant (I_{ω}) is defined as [5]:

$$I_{\omega} = I_{\omega} - z_c^2 I_z \quad (\text{A.15})$$

in which, I_{ω} is the classical warping constant used in Vlasov's model:

$$I_{\omega} = \int_A \omega^2 dA \quad (\text{A.16})$$

After development in the principal directions, this expression (I_{ω}) for three considered open hot-rolled sections is derived as:

- Doubly symmetric I section: (A.17)

$$I_{\omega} = \frac{1}{24} t_f \left(b_{f0}(\beta - 1) \left(\frac{x}{L} \right) + b_{f0} \right)^3 \left(d_0(\alpha - 1) \left(\frac{x}{L} \right) + d_0 - t_f \right)^2$$

- Singly symmetric I section:

$$I_{\omega} = \frac{t_f}{12} \left(1 + \left(\frac{b_{ft0}(\beta_t - 1) \left(\frac{x}{L} \right) + b_{ft0}}{b_{fb0}(\beta_b - 1) \left(\frac{x}{L} \right) + b_{fb0}} \right)^3 \right)^{-1} \times \left(d_0(\alpha - 1) \left(\frac{x}{L} \right) + d_0 - t_f \right)^2 \left(b_{ft0}(\beta_t - 1) \left(\frac{x}{L} \right) + b_{ft0} \right)^3 \quad (\text{A.18})$$

- Tee section:

$$I_{\omega} = \frac{t_f^3}{144} \left(b_{ft0}(\beta_t - 1) \left(\frac{x}{L} \right) + b_{ft0} \right)^3 + \frac{t_w^3}{36} \left(d_0(\alpha - 1) \left(\frac{x}{L} \right) + d_0 - t_f \right)^3 \quad (\text{A.19})$$

References

- [1] Achref, H., Foudil, M., Cherif, B., "Higher buckling and lateral buckling strength of unrestrained and braced thin-walled beams: Analytical, numerical and design approach applications", Journal of Constructional Steel Research, vol. 155, 2019, pp. 1-19.
- [2] Andrade, A., Camotim, D., "Lateral-torsional buckling of singly symmetric tapered beams, Theory and applications", Journal of Engineering Mechanics, ASCE, vol. 131(6), 2005, pp. 586-97.
- [3] Andrade, A., Camotim, D., Borges Dinis, P., "Lateral-torsional buckling of singly symmetric web-tapered thin-walled

- I-beams, 1D model vs. shell FEA”, *Computers and Structures*, vol. 85, 2007, pp. 1343-1359.
- [4] ANSYS, Version 5.4, Swanson Analysis System, Inc, 2007.
- [5] Asgarian, B., Soltani, M., Mohri, F., “Lateral-torsional buckling of tapered thin-walled beams with arbitrary cross-sections”, *Thin-Walled Structures*, vol. 62, 2013, pp. 96–108.
- [6] Attard, M.M., Kim, M-Y., “Lateral buckling of beams with shear deformations – A hyperelastic formulation”, *International Journal of Solids and Structures*; vol. 47, 2010, pp. 2825-2840.
- [7] Bazant, Z.P., Cedolin, L., “Stability of structures. Elastic, Inelastic, Fracture and Damage Theories”, New York, Dover Publications, (1991).
- [8] Benyamina, A.B, Meftah, S.A, Mohri, F., Daya, M., “Analytical solutions attempt for lateral torsional buckling of doubly symmetric web-tapered I-beams”, *Engineering structures*, vol. 56, 2013, pp. 1207-1219.
- [9] Brown, T.G., “Lateral-torsional buckling of tapered I-beams”, *Journal of the Structural Division, ASCE*, vol. 107(4), 1981, pp. 689-697.
- [10] Challamel N., Wang, C.M., “Exact lateral–torsional buckling solutions for cantilevered beams subjected to intermediate and end transverse point loads”, *Thin-Walled Structures*, vol. 48, 2010, pp. 71-76.
- [11] Chen, W.F., Lui, E.M., “Structural stability, theory and implementation”, New York, Elsevier, (1987).
- [12] Chen, H., Zhu, Y.F., Yao, Y., Huang, Y., “The finite element model research of the pre-twisted thin-walled beam”, *Structural Engineering and Mechanics*, vol. 57(3), 2016, pp. 389-402.
- [13] Chen, Z., Li, J., Sun, L., “Calculation of critical lateral-torsional buckling loads of beams subjected to arbitrarily transverse loads”, *International Journal of Structural Stability and Dynamics*, vol. 19(3), 2019, 1950031.
- [14] Erkmen, R.E., Mohareb, M., “Buckling analysis of thin-walled open members- A complementary energy variational principle”, *Thin-Walled Structures*, vol. 46, 2008, pp. 602–617.
- [15] Erkmen, R.E., Mohareb, M., “Buckling analysis of thin-walled open members- A Finite Element formulation”, *Thin-Walled Structures*, vol. 46, 2008, pp. 618–63.
- [16] Kabir, M.Z., Seif, A.E., “Lateral-torsional buckling of retrofitted steel I-beams using FRP sheets”, *Scientia Iranica-Transaction A: Civil Engineering*, vol. 17(4), 2010, pp. 262-272.
- [17] Kim, S-B, Kim, M-Y., “Improved formulation for spatial stability and free vibration of thin-walled tapered beams and space frames”, *Engineering Structures*, vol. 22, 2000, pp.446–458.
- [18] Kurniawan, C.W., Mahendran, M., “Elastic lateral buckling of simply supported Lite Steel beams subject to transverse loading”, *Thin-Walled Structures*, vol. 47, 2009, pp. 109-119.
- [19] Kuś, J., “Lateral-torsional buckling steel beams with simultaneously tapered flanges and web”, *Steel and Composite Structures*, vol. 19(4), 2015, pp. 897-916.
- [20] Lei, Z., Shu, T.G., “Lateral buckling of web-tapered I-beams: A new theory”, *Journal of Constructional Steel Research*, vol. 64, 2008, pp. 1379-1393.
- [21] Lezgy-Nazargah, M., “A generalized layered global-local beam theory for elasto-plastic analysis of thin-walled members”, *Thin-Walled Structures*, vol. 115, 2017, pp.48-57.
- [22] MATLAB Version 7.6.MathWorks Inc, USA, 2008.
- [23] Mohri, F., Damil, N., Ferry, M.P., “Linear and non-linear stability analyses of thin-walled beams with mono symmetric I sections”, *Thin-Walled Structures*, vol. 48, 2013, pp. 299–315.
- [24] Mohri, F., Meftah, S. A, Damil, N., “A large torsion beam Finite Element model for tapered thin-walled open cross-sections beams”, *Engineering Structures*, vol. 99, 2015, pp. 132-148.
- [25] Nguyen, T. T., Thang, P. T., Lee, J., “Flexural-torsional stability of thin-walled functionally graded open-section beams”, *Thin-Walled Structures*, vol. 110, 2017, pp. 88-96.
- [26] Nguyen, T. T., Thang, P. T., Lee, J., “Lateral buckling analysis of thin-walled functionally graded open-section beams”, *Composite Structures*, vol. 160, 2017, pp. 952-963.
- [27] Pasquino, M., Sciarra, F.M., “Buckling of thin-walled beams with open and generally variable section”, *Computers and Structures*, vol. 44, 1992, pp. 843-849.
- [28] Rao, C. K., Rao, L. B., “Torsional post-buckling of thin-walled open section clamped beam supported on Winkler-Pasternak foundation”, *Thin-Walled Structures*, vol. 116, 2017, pp. 320-325.
- [29] Ruta, P., Szybinski, J., “Lateral stability of bending non-prismatic thin-walled beams using orthogonal series”, *Procedia Engineering*, vol. 11, 2015, pp. 694-701.
- [30] Soltani, M., Asgarian, B., Mohri, F., “Elastic instability and free vibration analyses of tapered thin-walled beams by the power series method”, *Journal of constructional steel research*, vol. 96, 2014, pp. 106-126.
- [31] Soltani, M., Asgarian, B., Mohri, F., “Finite Element method for stability and free vibration analyses of non-prismatic thin-walled beams”, *Thin-Walled Structures*, vol. 82, 2014, pp. 245-261.
- [32] Soltani, M., Asgarian, B., Mohri, F., “Improved finite element model for lateral stability analysis of axially functionally graded non-prismatic I-beams”, *International Journal of Structural Stability and Dynamics*, vol. 19(9), 2019, 1950108.
- [33] Tan, M., Cheng, W., “Non-linear lateral buckling analysis of unequal thickness thin-walled box beam under an eccentric load”, *Thin-Walled Structures*, vol. 139, 2019, pp.77-90.
- [34] Timoshenko, S.P., Gere, J.M., “Theory of elastic stability”, 2nd Ed. New York, McGraw-Hill, (1961).
- [35] Vlasov, V.Z., “Thin-walled elastic beams”, Moscow, 1959. French translation, Pièces longues en voiles minces, Eyrolles, Paris, (1962).
- [36] Yang, Y.B, Yau, J.D, “Stability of beams with tapered I-sections”, *Journal of Engineering Mechanics, ASCE*, vol. 113(9), 1987, pp.1337-1357.
- [37] Yau, J.D., “Stability of tapered I-Beams under torsional moments”, *Finite Elements in Analysis and Design*, vol. 42, 2006, pp. 914-927.
- [38] Yuan, W.B., Kim, B., Chen, C., “Lateral–torsional buckling of steel web tapered tee-section cantilevers”, *Journal of Constructional Steel Research*, vol. 87, 2013, pp. 31–37.